

RESEARCH ARTICLE

10.1002/2015WR018515

Backward fractional advection dispersion model for contaminant source prediction

Yong Zhang¹, Mark M. Meerschaert², and Roseanna M. Neupauer³

Key Points:

- Backward model for superdiffusion governed by fractional-derivative equations is not self-adjoint
- Probability distribution of source location for superdiffusion is skewed in the upstream direction
- Backward model with a range of percentiles can identify source and release time at MADE-2 site

Correspondence to:

Y. Zhang,
yzhang264@ua.edu

Citation:

Zhang, Y., M. M. Meerschaert, and R. M. Neupauer (2016), Backward fractional advection dispersion model for contaminant source prediction, *Water Resour. Res.*, 52, 2462–2473, doi:10.1002/2015WR018515.

Received 4 JAN 2016

Accepted 9 MAR 2016

Accepted article online 14 MAR 2016

Published online 1 APR 2016

¹Department of Geological Sciences, University of Alabama, Tuscaloosa, Alabama, USA, ²Department of Statistics and Probability, Michigan State University, East Lansing, Michigan, USA, ³Department of Civil, Environmental, and Architectural Engineering, University of Colorado, Boulder, Colorado, USA

Abstract The forward Fractional Advection Dispersion Equation (FADE) provides a useful model for non-Fickian transport in heterogeneous porous media. The space FADE captures the long leading tail, skewness, and fast spreading typically seen in concentration profiles from field data. This paper develops the corresponding backward FADE model, to identify source location and release time. The backward method is developed from the theory of inverse problems, and then explained from a stochastic point of view. The resultant backward FADE differs significantly from the traditional backward Advection Dispersion Equation (ADE) because the fractional derivative is not self-adjoint and the probability density function for backward locations is highly skewed. Finally, the method is validated using tracer data from a well-known field experiment, where the peak of the backward FADE curve predicts source release time, while the median or a range of percentiles can be used to determine the most likely source location for the observed plume. The backward ADE cannot reliably identify the source in this application, since the forward ADE does not provide an adequate fit to the concentration data.

1. Introduction

The Advection Dispersion Equation (ADE) model built upon the assumption of Fick's first law quantifies well tracer transport in homogeneous media. Conservative tracer transport in heterogeneous systems however was well documented to be non-Fickian and cannot be conveniently modeled by the ADE [Berkowitz *et al.*, 2006], motivating the application of alternative transport models such as the space Fractional Advection Dispersion Equation (FADE) [Metzler and Klafter, 2000, 2004]. The space FADE assumes power law distribution for tracer velocity and captures superdiffusive transport where the plume variance grows faster than linear in time [Benson, 1998; Zhang *et al.*, 2009; Schumer *et al.*, 2009]. The FADE models have been applied to a wide variety of problems in science and engineering, including river flows [Deng *et al.*, 2006; Kim and Kavvas, 2006; Meerschaert *et al.*, 2008; Zhang *et al.*, 2007, 2012], landscape evolution [Schumer *et al.*, 2009; Voller *et al.*, 2012], and contaminant transport in highly heterogeneous aquifers [Benson, 1998; Benson *et al.*, 2001; Meerschaert and Sikorskii, 2012]. In this model for groundwater flow, the second spatial derivative in the traditional ADE is replaced by a fractional derivative of order α , where $1 < \alpha < 2$. Point source solutions of the FADE exhibit a long leading tail, positive skewness, and faster spreading than the ADE. The FADE has been shown to provide a superior fit to laboratory experiments and field data [Meerschaert *et al.*, 2008; Zhang *et al.*, 2009]. Hence the results presented here should be widely applicable.

Groundwater contaminant source identification is needed for groundwater management and remediation. For example, source removal, remedial strategy design and evaluation, and identification of responsible parties may require information for source location and/or release history. Although both forward and backward models can identify a contaminant source, the forward model requires repeated simulations for each specified source while the backward model provides the probability for all upstream locations given each detection. Backward modeling therefore is computationally more efficient if the number of sources is more than the number of detections [Neupauer and Wilson, 1999]. Various backward models had been developed based on the assumption of Fickian diffusion for contaminants; see the extensive review by Atmadja and Bagtzoglou [2001]. As discussed above, conservative tracer transport in heterogeneous media is typically non-Fickian and requires nonlocal transport models such as the FADE.

The inverse FADE model however remains unknown. Similar to its ADE counterpart, the inverse problem for the FADE resolves the source location or time from measured concentration data at a later time. This ill-posed problem was recently considered by repeated forward modeling, varying the initial conditions to develop a picture of the likely source [Jia et al., 2015]. A more efficient approach was proposed by Neupauer and Wilson [2002] for the traditional ADE. The method computes the marginal sensitivity of a performance measure representing the likelihood of source location or time, with respect to the total plume mass, via the adjoint method. This paper carries out the same calculations for the FADE model to provide an efficient solution to the inverse source location problem underlying superdiffusive anomalous transport.

The rest of the paper is organized as follows. The backward FADE model is derived in section 2 by combining the fractional-adjoint formula and the sensitivity analysis approach. Stochastic processes underlying the resultant backward FADE model and its forward counterpart are then interpreted, as well as the traditional ADE model, in section 3. One field application is shown in section 4. Model extensions and comparisons are then discussed in section 5, followed by conclusions in section 6. Mathematical details are collected in Appendix A.

2. Derivation of the Backward FADE

The space FADE for tracer concentration $C(x, t)$ at location x at time t is given by [Meerschaert et al., 1999; Zhang et al., 2007]

$$\frac{\partial}{\partial t} [\theta C] = -\frac{\partial}{\partial x} [\theta v C] + \frac{\partial}{\partial x} \left[\theta D \frac{\partial^{\alpha-1} C}{\partial x^{\alpha-1}} \right] + q_i C_i - q_o C, \tag{1}$$

where the index α ($1 < \alpha \leq 2$) represents the order of the fractional derivative, x denotes the spatial coordinate ($-\infty < x < +\infty$), q_i is the source inflow rate, q_o is the sink outflow rate, C_i is the inflow concentration, and the point source initial condition $C(x, 0) = M_0 \delta(x - x_0) / \theta$ (here M_0 is the initial mass). The seepage velocity v , effective dispersion coefficient D , and effective porosity θ may vary with the location x . When $\alpha = 2$, equation (1) reduces to the traditional ADE. In hydrologic sciences, the FADE (1) was developed to model superdiffusive plumes in highly heterogeneous aquifers [Benson, 1998; Benson et al., 2001; Zhang et al., 2007; Meerschaert and Sikorskii, 2012]; see further discussion in the next section.

We then apply the sensitivity analysis approach proposed by Neupauer and Wilson [2002], using a fractional adjoint formula to derive the backward FADE. The marginal sensitivity of a performance measure P with respect to M_0 is [see Neupauer and Wilson, 2002, equation (11)]:

$$\frac{dP}{dM_0} = \int_{-\infty}^{+\infty} \int_0^T \frac{\partial h(M_0, C)}{\partial C} \frac{\partial C}{\partial M_0} dx dt, \tag{2}$$

where the function $h(M_0, C)$ is called the “performance functional.” For location probability, h is related to resident concentration at the detection location and time, given by $h = C \delta(x - x_d) \delta(\tau)$ where x_d is the detection location and the backward time $\tau = T - t$, where T is the detection time [Neupauer and Wilson, 1999, 2002].

The governing equation for the state sensitivity $\phi = \partial C / \partial M_0$ can then be obtained by differentiating each term of (1) with respect to the system parameter M_0 , which yields:

$$\frac{\partial}{\partial t} (\theta \phi) = -\frac{\partial}{\partial x} (\theta v \phi) + \frac{\partial}{\partial x} \left(\theta D \frac{\partial^{\alpha-1} \phi}{\partial x^{\alpha-1}} \right) - q_o \phi, \tag{3}$$

with initial condition $\phi(x, 0) = \delta(x - x_0) / \theta$, noting that the derivative dC/dM_0 commutes with the integer order and fractional order spatial x derivatives. Take the inner product of (3) with an arbitrary function $A(x, t)$, the adjoint state, to get

$$\int_0^T \int_{-\infty}^{+\infty} A \left[\frac{\partial}{\partial t} (\theta \phi) + \frac{\partial (\theta v \phi)}{\partial x} - \frac{\partial}{\partial x} \left(\theta D \frac{\partial^{\alpha-1} \phi}{\partial x^{\alpha-1}} \right) + q_o \phi \right] dx dt = 0. \tag{4}$$

Apply the adjoint formula

$$\int_{-\infty}^{+\infty} g(x) \frac{\partial^{x-1} f(x)}{\partial x^{x-1}} dx = \int_{-\infty}^{+\infty} f(x) \frac{\partial^{x-1} g(x)}{\partial (-x)^{x-1}} dx, \tag{5}$$

in Zhang et al. [2006, Appendix A] (or apply the fractional integration by parts formula from Polyanin and Manzhirov [1998], noting that these probability density functions vanish at infinity) to get

$$\int_0^T \int_{-\infty}^{+\infty} \left[-\theta \phi \frac{\partial A}{\partial t} - \theta v \phi \frac{\partial A}{\partial x} + \phi \frac{\partial^{x-1}}{\partial (-x)^{x-1}} \left(\theta D \frac{\partial A}{\partial x} \right) + q_o \phi A \right] dx dt + \int_{-\infty}^{+\infty} A \theta \phi \Big|_{t=0}^{t=T} dx = 0. \tag{6}$$

Now subtract (6) from (2) to get

$$\frac{dP}{dM_0} = \int_{-\infty}^{+\infty} \int_0^T \phi \left[\frac{\partial h}{\partial C} + \theta \frac{\partial A}{\partial t} + v \theta \frac{\partial A}{\partial x} - \frac{\partial^{x-1}}{\partial (-x)^{x-1}} \left(\theta D \frac{\partial A}{\partial x} \right) - q_o A \right] dx dt - \int_{-\infty}^{+\infty} A \theta \phi \Big|_{t=0}^{t=T} dx, \tag{7}$$

and choose the adjoint state A such that the first integral in (7) equals zero. Then we obtain the following governing equation for A

$$\theta \frac{\partial A}{\partial t} = -v \theta \frac{\partial A}{\partial x} + \frac{\partial^{x-1}}{\partial (-x)^{x-1}} \left(\theta D \frac{\partial A}{\partial x} \right) + q_o A - \frac{\partial h}{\partial C}. \tag{8}$$

A change of variables $\tau = T - t$ yields the adjoint equation for the FADE (1) in terms of the backward time τ

$$\frac{\partial}{\partial \tau} (\theta A) = \frac{\partial}{\partial x} (v \theta A) - \frac{\partial^{x-1}}{\partial (-x)^{x-1}} \left[\theta D \frac{\partial A}{\partial x} \right] - q_l A + \frac{\partial h}{\partial C}, \tag{9}$$

where (1) we have replaced the outflow rate q_o by the inflow rate q_l since we assume steady state flow: $A \partial(\theta v)/\partial x = A(q_l - q_o)$, and (2) we assume that the porosity θ does not change with time. Since $\partial/\partial(-x) = -\partial/\partial x$, we can also write this equation in the form

$$\frac{\partial}{\partial \tau} (\theta A) = \frac{\partial}{\partial x} (v \theta A) + \frac{\partial^{x-1}}{\partial (-x)^{x-1}} \left[\theta D \frac{\partial A}{\partial (-x)} \right] - q_l A + \frac{\partial h}{\partial C}. \tag{10}$$

If θ and D are constants independent of x , since

$$\frac{\partial^{x-1}}{\partial (-x)^{x-1}} \frac{\partial}{\partial (-x)} = \frac{\partial^x}{\partial (-x)^x}$$

we can rewrite the backward FADE (10) in the constant coefficient case as

$$\frac{\partial A}{\partial \tau} = v \frac{\partial A}{\partial x} + D \frac{\partial^x A}{\partial (-x)^x} - \frac{q_l}{\theta} A + \frac{1}{\theta} \frac{\partial h}{\partial C}. \tag{11}$$

This is just the forward FADE with the velocity reversed, and the positive fractional-derivative turned negative.

The inverse FADE model (10) and its simplified version (11) are the main findings of this study.

3. Stochastic Explanation of the Physical Models: FADE Versus ADE

The space FADE and the ADE describe different random processes. On the one hand, it is well known that the ADE solution equals the density of Brownian motion with drift. Point source solutions of the ADE are given by a normal probability density, consistent with the central limit theorem for a sum of independent particle motions. On the other hand, the FADE relates to a heavy-tailed random walk, where the probability of a particle moving x units downstream falls off like $x^{-\alpha}$ for long distances. Point source solutions are given by an α -stable probability density, consistent with the Kolmogorov-Feller extended central limit theorem [Meerschaert, 2012; Meerschaert and Sikorskii, 2012].

The space FADE captures superdiffusive transport in a medium with preferential flow paths. In a complex porous medium, particle velocities are highly variable, ranging over several orders of magnitude, and typically following a power law distribution. A small fraction of particles follow a fast path, causing enhanced

plume spreading and a thicker leading tail. Without taking this highly variable velocity field into account, the traditional ADE can underpredict concentrations at the leading plume edge by several orders of magnitude [Benson et al., 2001]. Solomon et al. [1993] explain how power law velocities in turbulent flow lead to Lévy flights, and these are governed by the same FADE equation. Shlesinger et al. [1993] describe how Lévy flights are used to model a variety of chaotic dynamical systems. Hence the methods developed here may have wide applicability to geophysical phenomena involving complex, chaotic dynamics.

The backward FADE and ADE models differ in the dispersion term. The random walk underlying the backward model reverses the forward particle motions, tracking them back in time to their most likely source. The backward ADE (with constant velocity and dispersivity) corresponds to the forward ADE with the velocity reversed. Neupauer and Wilson [2002] showed that the backward ADE model is:

$$\frac{\partial}{\partial t}(\theta A) = \frac{\partial}{\partial x}(\theta v A) + \frac{\partial}{\partial x} \left[\theta D \frac{\partial A}{\partial x} \right] - q_1 A + \frac{\partial h}{\partial C} \tag{12}$$

where the dispersion term is the same forward and backward, since the second derivative in the ADE is self-adjoint. This is because, in the ADE, particle motions follow a velocity $v > 0$ plus a symmetric dispersion (representing deviations from the mean velocity) that is just as likely to jump forward as backward, with the same (normal) distribution. Hence the reversed process has an opposite velocity, but the same dispersion. Probabilistically, the underlying random walk consists of regular particle movements perturbed by a symmetric random disturbance.

This paper shows that the FADE is fundamentally different. Physically, the forward FADE (1) models transport at velocity $v > 0$ indicating left-to-right movements, plus dispersion characterized by left-to-right particle displacements with a power law distribution, representing wide variations in velocity in a heterogeneous porous medium. The likelihood of a jump larger than x units forward declines as a power law function, and the accumulated jumps are then centered to mean zero to model the dispersion. See section 3.5 in the recent book of Meerschaert and Sikorskii [2012] for complete details, or Meerschaert [2012] for a quick summary. In the same manner, the backward FADE (11) models transport at velocity, v , indicating right-to-left movements, and particle displacements with the same distribution, but with the direction reversed. The adjoint of the positive fractional derivative in the FADE is a negative fractional derivative of the same order α . The long downstream jumps in the forward random walk model become long upstream jumps in the backward model. Hence the backward probability profile shows a long left tail (which can be seen in applications in the next section), representing increased uncertainty upstream.

It is also noteworthy that, when $\alpha = 2$, the backward FADE model (10) reduces to the backward ADE model (12), as expected. The backward ADE and FADE models will be further discussed and compared below.

4. Application to the MADE Site

The well-known MADE-2 tracer test conducted in Mississippi involved an 11 m thick alluvial aquifer consisting of gravel/sand lenses (up to 8 m long) with minor amounts of silt and clay [Boggs et al., 1992; Boggs and Adams, 1992; Adams and Gelhar, 1992; Rehfeldt et al., 1992]. Tritium was injected, which can be simplified as an instantaneous point source, and then concentrations were measured downstream to form snapshots of the concentration profile.

A previous study [Benson et al., 2001] demonstrated how the forward FADE with constant coefficients effectively captures the long leading tail and fast spreading observed in this data. For that study, the fractional index $\alpha = 1.1$, average groundwater velocity $v = 0.12$ m/d, and fractional dispersion coefficient $D = 0.14$ m²/d were estimated using the sample mean permeability, field-measured groundwater velocities, and the general head gradient. Figure 1 illustrates the model fit using these parameter values, along with the measured concentration values at day 132, 224, and 328. The logarithmic scale on the vertical axis was selected to clarify the fit on the right (downstream) tail.

It is well known that the ADE model with constant coefficients cannot capture the superdiffusion observed at the MADE site; see for example, the extensive review by Zheng et al. [2011]. Therefore, the ADE model is not the focus of this section, and the application of the inverse ADE model (12) will only be shown briefly in section 5.3 for model comparison.

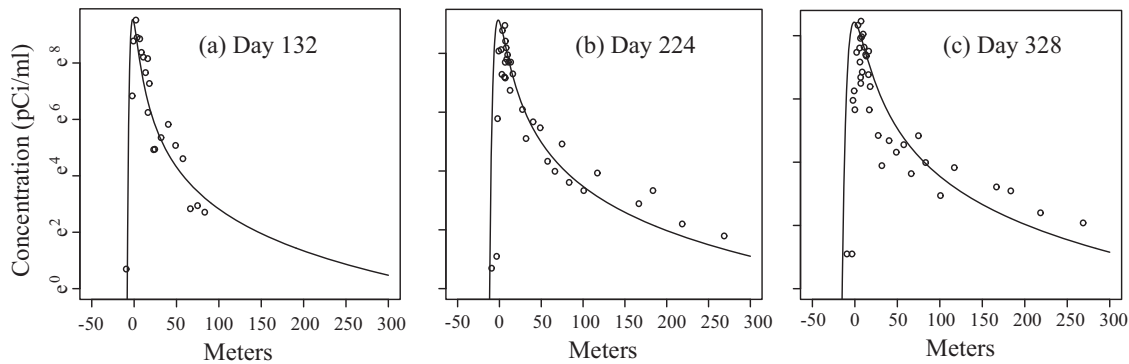


Figure 1. The MADE-2 tritium plume data (circles) and a forward FADE model (1) with constant θ , $\alpha = 1.1$, $\nu = 0.12$, and $D = 0.14$ that captures the leading tail and spreading rate at Day (a) 132, (b) 224, and (c) 328.

4.1. Backward Location Probability Density Function (PDF) for Superdiffusion

To calculate the probability density function $f_x(x; \tau)$ of upstream location x for a contaminant release, given an observed contaminant at location $x = x_d$ at time $\tau = 0$, use the same performance functional $h = C\delta(x - x_d)\delta(\tau)$ as in Neupauer and Wilson [2002, equation (9)] so that $\partial h / \partial C = \delta(x - x_d)\delta(\tau)$ and $q_l = 0$ in (11). The governing equation for the backward location PDF is therefore

$$\frac{\partial f_x(x; \tau)}{\partial \tau} = \nu \frac{\partial f_x(x; \tau)}{\partial x} + D \frac{\partial^2 f_x(x; \tau)}{\partial (-x)^\alpha} + \delta(x - x_d)\delta(\tau), \tag{13}$$

where the PDF f relates to the adjoint state A in (11) via the formula $f_x(x; \tau) = \theta A(x, \tau)$ (here θ is constant). Note that in the notation of the backward location PDF $f_x(x; \tau)$, variables to the left of the semicolon (i.e., x) are random variables, and variables to the right of the semicolon (i.e., τ) are deterministic parameters. The same rule in notation will be used below for the backward travel time PDF. The analytical solution of (13) is $f_x(x; \tau) = p_x(\beta, \sigma, \mu)$ with $\mu = \nu\tau$, $\beta = -1$, and $\sigma^2 = D\tau|\cos(\pi\alpha/2)|$, where the stable probability density function $p_x(\beta, \sigma, \mu)$ can be computed using freely available statistical software, see Meerschaert and Sikorskii [2012, chapter 5].

We plot $f_x(x; \tau)$ to predict the location of a contaminant release, starting at the observed peak concentration, and fixing the elapsed time of $\tau = 132, 224,$ and 328 days, respectively. The results in Figure 2 are negatively skewed, reflecting the fact that the reversed particle flow has particles jumping back upstream as time runs backward. The true release location (vertical bar) lies to the left of the peak in this highly skewed probability density and in all cases lies between the mean and the median of the curve (see Table 1). The peak lies at the 28th percentile, and the mean at the 90th or 91st percentile, in all three cases. The second-highest concentration measured (not the model simulation result) on day 328 occurs 3.6 m downstream, and based on this starting data, the true source location is at the 47th percentile, very close to the median.

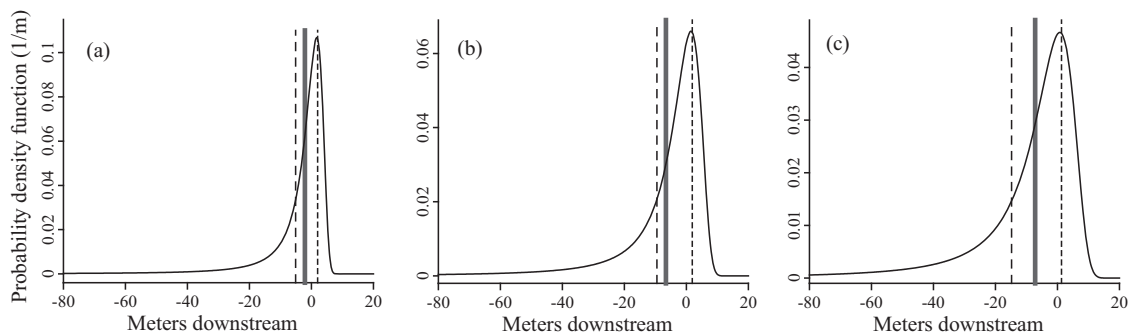


Figure 2. Backward FADE (11) prediction of contaminant release location, starting at peak concentration of the MADE-2 plume for Day (a) 132, (b) 224, and (c) 328 with constant porosity θ , index $\alpha = 1.1$, velocity $\nu = 0.12$ m/d, and dispersion coefficient $D = 0.14$ m²/d. Vertical solid bar shows true release location. The long and short dashed lines show the 75th and 25th percentiles, respectively. Note that this figure is a probabilistic representation of location.

Table 1. The Measured and Predicted Source Location for the MADE-2 Tracer Test (Shown in Figure 2), Where the Observation Is the Measured Plume Peak Shown in Figure 1^a

t (days)	Observed Peak (m)	Predicted Mean (m)	Predicted Median (m)	P _{25th} (m)	P _{75th} (m)	P _{Observed Peak} (%)
132	2.1	15.84	0.6	-2.0	5.1	61st
224	6.6	26.88	2.2	-1.9	9.5	67th
328	7.2	39.36	4.5	-1.3	14.8	59th

^a“Observed Peak” denotes the true source location, P_{25th} and P_{75th} denote the 25th and 75th Percentiles, and P_{Observed Peak} denotes the percentile of the observed peak.

4.2. Backward Travel Time Probability Density Function for Superdiffusion

To compute the PDF $f_{\tau}(\tau; x)$ of contaminant release time τ (i.e., the backward travel time PDF), rewrite Zhang *et al.* [2006, equation (8)] using equation (7) in the same paper to get

$$C^f = C - \frac{D \partial^{x-1} C}{v \partial x^{x-1}}, \quad (14)$$

and then extend Neupauer and Wilson [2002, equation (19)] to the fractional case using (5) to get the load function

$$\frac{\partial h}{\partial C} = \delta(x - x_d) \delta(\tau) + \frac{D \partial^{x-1} \delta(x - x_d)}{v \partial (-x)^{x-1}} \delta(\tau). \quad (15)$$

Argue as in Zhang *et al.* [2006, equation (8)] that the solution to (11) with load function (15) and $q_l = 0$ is given by $f_x(x; \tau) + (x + v\tau)f_x(x; \tau)/(v\alpha\tau)$. Then apply Neupauer and Wilson [2002, equation (23)] with $q = v\theta$ (where q is the Darcy velocity) to see that

$$f_{\tau}(\tau; x) = v \left[1 + \frac{x + v\tau}{v\alpha\tau} \right] f_x(x; \tau). \quad (16)$$

The derivation of solution (16) and validation of formulas (14) and (15) are shown in Appendix A for interested readers.

We plot (16) to demonstrate the effectiveness of this model for determining the time of a contaminant release, starting from an observed contaminant at location $x = x_d$ at time $\tau = 0$. For this study, we select the monitoring well located at the plume peak for each snapshot (see Table 1) as the initial data for the backward FADE. The results in Figure 3 show that the backward FADE provides a reasonably accurate prediction of release time, using the same model parameters fit by Benson *et al.* [2001] for the forward prediction problem.

5. Discussion

Here we discuss estimation of source location using the backward FADE model and potential extensions of the backward model. We then compare the backward PDFs for superdiffusive (FADE) and normal-diffusive (ADE) transport.

5.1. Estimation of the Source Location

The backward FADE provides a reasonably accurate estimate of source release time, as seen in Figure 3. The predicted source location in Figure 2 is more variable, and the interpretation of this curve requires some

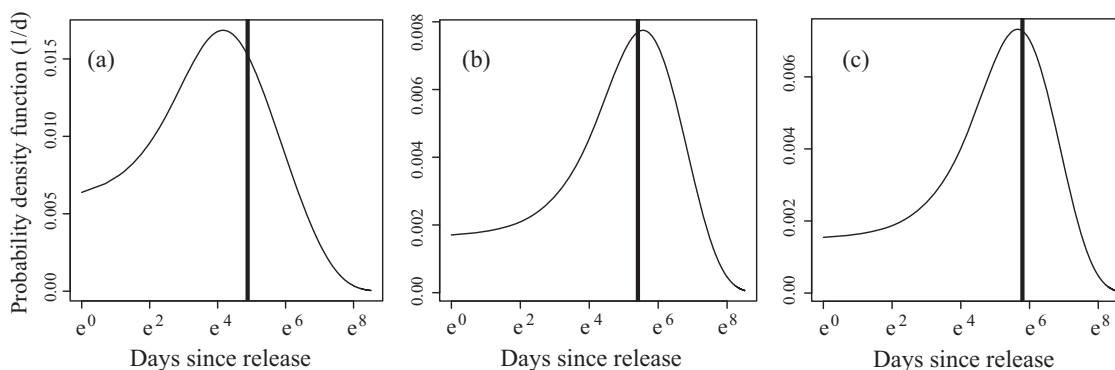


Figure 3. Backward FADE (11) prediction of contaminant release time, starting at peak concentration of the MADE-2 plume for Day (a) 132, (b) 224, and (c) 328 with constant porosity θ , index $\alpha = 1.1$, velocity $v = 0.12$ m/d, and dispersion coefficient $D = 0.14$ m²/d. Vertical bar shows true release time.

care. Since the probability curve is highly skewed to the left, its mean lies far to the left of its peak, with the median in between. Of these three basic descriptors, the median provides the best point estimate of the source location. A reasonable interval estimate is given by the 25th and 75th percentiles, and the actual source location was found to lie between these values in all cases.

Note that this conclusion does not imply that the FADE model is not appropriate for the MADE-2 tritium transport. It actually implies that specific treatment is needed when identifying source for pollutant undergoing superdiffusion, which differs from normal diffusion in homogeneous media. If the well located at the plume peak is selected as the single detection for source identification, the median or a range of percentiles in the backward location PDF is needed to account for the skewed PDF curve due to superdiffusion.

5.2. Model Extension

The backward FADE (10) with spatially varying coefficients θ , v , and D can be solved by a finite difference method [Tadjeran *et al.*, 2006] or by particle tracking [Zhang *et al.*, 2006]. Some faster numerical methods are also available [Chen and Deng, 2014; Wang and Yang, 2013; Zayernouri and Karniadakis, 2014] for problems on an unbounded domain. Fractional diffusion on a bounded domain represents a challenging problem. A bounded domain is needed in hydrological applications where contaminant may experience a reflecting or absorbing barrier, a mass sink, or an inflowing boundary. The issues with simulation include: (1) fractional boundary conditions and fractional-derivative models remain to be shown [Deftterli *et al.*, 2015], and (2) numerical solvers are not developed yet. We will focus on these challenges in a future study.

A vector FADE has also been applied to model groundwater plumes in higher dimensions [Zhang *et al.*, 2007], a time-fractional ADE has been proposed to model retention at the source [Schumer *et al.*, 2003], and a tempered FADE was used to reduce the extreme power law tails [Meerschaert *et al.*, 2008; Sabzikar *et al.*, 2015]. It would also be interesting to derive the corresponding backward models, which will be explored in future studies (since none of them are simple extensions of the results presented here).

The inverse model and solutions developed in this paper may also be generally applicable to the inverse modeling of other geophysical and ecological dynamics, such as toxic waste disposal, indoor contamination and gaseous emission, nutrient export from watersheds, and sediment in rivers whose transport can be dominated by non-Fickian dispersion due to the intrinsic multiscale medium heterogeneity [Liu and Zhai, 2007; Zhang *et al.*, 2012]. Further validation and applications of the inverse FADE model are therefore needed.

The backward FADE (10) and PDFs are developed for an instantaneous, point source. Modifications are needed for a nonpoint and/or continuous source. For example, for a nonpoint source, the backward travel time PDF can be integrated over the known spatial domain of the source. For an unusual case where the location of the nonpoint source is unknown and the shape of the region is known (such as a 100 m \times 100 m square), we can calculate the moving average of backward location PDF (of a 100 m \times 100 m window) at a given backward time. In addition, to identify the position (or release history) for a continuous source such as a leaking underground storage tank, the backward location (or travel time) PDF might be conditioned on the observed contaminant breakthrough curve at the detection well. We will test the above extension in a future study.

5.3. Model Comparison

To distinguish the impact of Fickian and non-Fickian transport on real-world contaminant source identification, we apply both the backward FADE (11) and the backward ADE (12) with constant coefficients to identify the MADE-2 tracer source. We will also use a slightly different FADE parameterization, to study model sensitivity.

The velocity v and dispersion coefficient D in the forward FADE (1) are now fitted using the plume mean and variance measured at the MADE-1 tracer test [Adams and Gelhar, 1992] (Figures 4a and 4b), using the spatial moment formulae given in Zhang *et al.* [2008]. With a truncation due to the furthest monitoring well at the MADE site, the plume mean and variance are well defined. This fitting exercise results in parameters $v = 0.14$ m/d and $D = 0.12$ m²/d, where the best fit velocity lies in the low end of the field measured velocity (0.12–0.36 m/d). These parameters differ slightly from those used in section 4 where v and D were predicted given other field measurements.

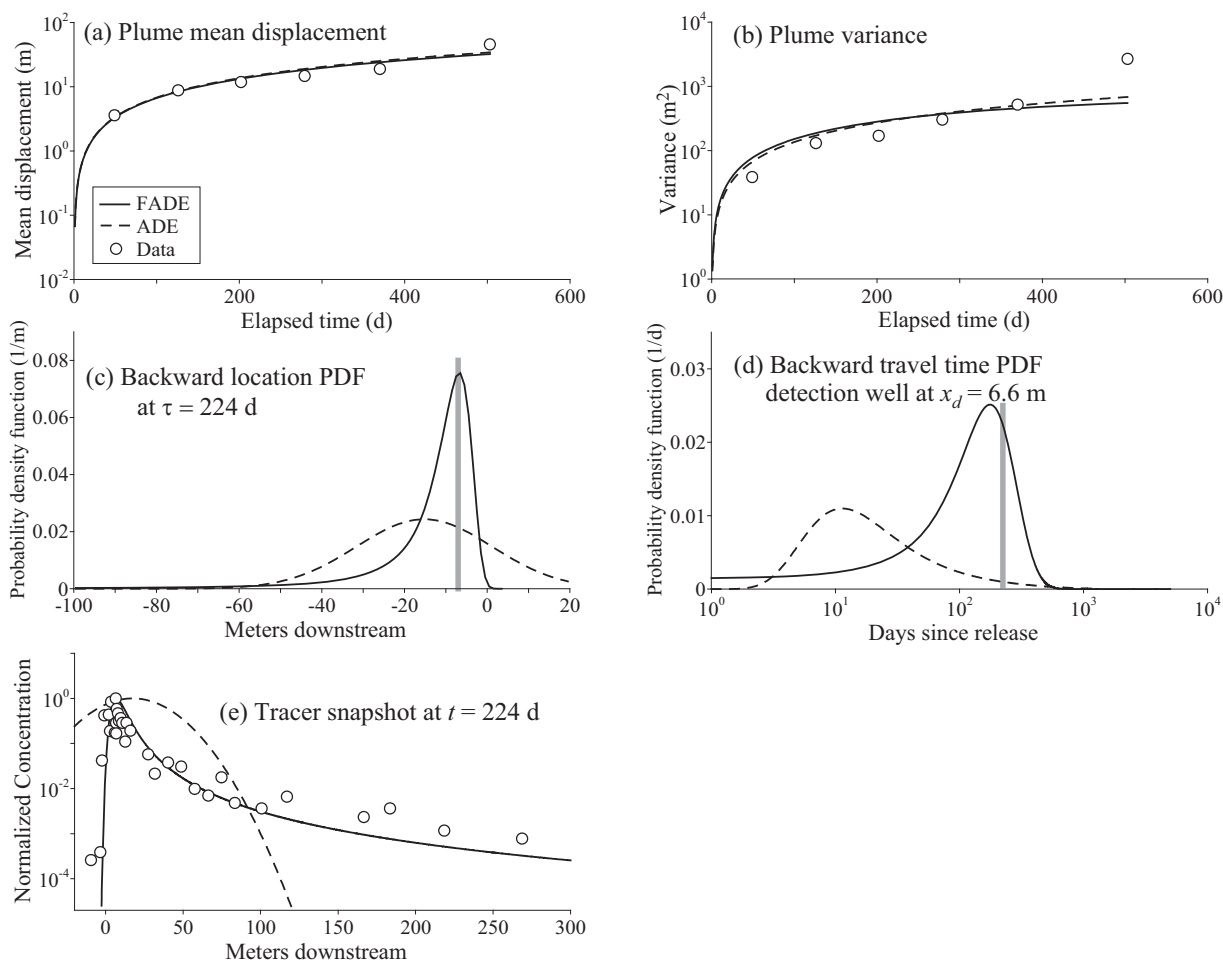


Figure 4. Application for MADE tracer tests: the measured versus the best fit (a) mean and (b) variance of tracer displacement using the FADE (1) and the standard ADE, taking into account the finite model domain. (c) The predicted backward location PDF using the inverse FADE (11) and the inverse ADE (12) at backward time 224 days. (d) Predicted backward travel time PDF for the detection well at $x_d = 6.6$ m downstream from the source. (e) The fitted ADE and FADE models at Day 224 along with the observed concentration data. The vertical bar shows the actual point source location in Figure 4c and the true release time in Figure 4d.

For comparison purposes, we also fit the same data using the standard ADE model $\partial C/\partial t = -v\partial C/\partial x + D\partial^2 C/\partial x^2$. The resultant constant parameters for the ADE are: $v = 0.068$ m/d and $D = 0.68$ m/d, where the longitudinal dispersivity is the same order as that calculated by *Adams and Gelhar* [1992].

The predicted backward travel time PDF using (11) generally matches the true release time; see Figure 4d for one example. The peak of the predicted backward location PDF using (11) is close to the true source location at day 224, and the true release location is at the 27th percentile of the distribution (Figure 4c).

The backward ADE, however, gives a poor estimate for both the source position (dashed line in Figure 4c) and release time (Figure 4d). For a Fickian-based model to capture the fast growing plume variance observed at the MADE site (Figure 4b), a large dispersion coefficient is required, increasing the prediction uncertainty across a wide domain in backward location and travel time. Although the ADE model with constant parameters can capture the observed plume variance, Fickian diffusion cannot efficiently capture the positively skewed plume snapshot (Figure 4e). Therefore, the Fickian-based ADE model may not provide a reasonable identification of contaminant source if superdiffusion is apparent in contaminant transport.

6. Conclusions

This paper derives and tests a backward Fractional Advection Dispersion Equation (FADE) model for superdiffusive transport in heterogeneous geological media. The model provides probabilistic estimates for the

source location and release time. Adjoint-based sensitivity analysis is used to derive the inverse model on an unbounded domain, a stochastic interpretation is discussed, and an example application is presented. The combined theoretical analysis and practical application lead to three main conclusions.

First, the backward FADE is fundamentally different from the traditional backward ADE, because the fractional derivative is not self-adjoint. The backward FADE model not only reverses the flow velocity, but also turns the positive fractional derivative in the forward model to the negative fractional derivative. The positively skewed α -stable probability density describing forward particle jumps results in the negatively skewed stable density for backward PDFs. The dispersion term is not self-adjoint unless the index in the FADE model approaches two (i.e., the FADE reduces to the ADE). In the backward ADE model, the dispersion term remains unchanged because of the symmetric Fickian diffusion; i.e., particles jump forward and backward (due to deviations from the mean velocity) with the same probability (and magnitude if the dispersion coefficient is space independent).

Second, the probability distribution of likely source locations predicted by the backward FADE model is highly skewed in the upstream direction. Therefore, if a single observation is used, the median is a more reliable predictor of source location than either the peak or the mean. A range of percentiles (i.e., from the 25th to 75th percentiles) can also be used. For source release time, the peak of the backward FADE curve seems to provide a reasonable predictor.

Third, comparisons show that the backward ADE cannot reliably identify source location and release time for the MADE-2 tracer. This is not a surprise, since although the forward ADE model can capture the overall trend of mean displacement and variance of plumes, Fickian transport has an intrinsic limitation in characterizing the positive skewness of plume snapshots observed for almost all MADE site tracers. Hence the source of contaminants exhibiting non-Fickian dynamics in real aquifers may be better identified by nonlocal transport models such as the backward FADE developed by this study.

Appendix A: Relationship Between Backward Travel Time PDF and Backward Location PDF for Superdiffusion

A1. Derivation of Equation (14)

Consider the forward-in-time FADE with constant parameters

$$\frac{\partial C(x, t)}{\partial t} = -v \frac{\partial C(x, t)}{\partial x} + D \frac{\partial^\alpha C(x, t)}{\partial x^\alpha}$$

with a point source initial condition $C(x, 0) = \delta(x)$. Here C represents the resident concentration, which is related to the flux concentration C^f .

Zhang *et al.* [2006] showed that the Fourier ($x \rightarrow k$) and Laplace ($t \rightarrow s$) transform of the flux concentration is given by

$$\tilde{\hat{C}}^f(k, s) = \int_{-\infty}^{\infty} \int_0^{\infty} e^{-ikx} e^{-st} C^f(x, t) dt dx = \frac{1}{v} \frac{v - D(ik)^{\alpha-1}}{s + ikv - D(ik)^\alpha}, \quad (A1)$$

where the tilde and the hat represent the Laplace and the Fourier transform, respectively. The Fourier-Laplace transform of the resident concentration is given by

$$\tilde{\hat{C}}(k, s) = \frac{1}{s + ikv - D(ik)^\alpha}, \quad (A2)$$

which is in Zhang *et al.* [2006, equation (5)]. Combining (A1) and (A2), one obtains

$$v\alpha \tilde{\hat{C}}^f(k, s) + v(1-\alpha) \tilde{\hat{C}}(k, s) = \frac{v - D\alpha(ik)^{\alpha-1}}{s + ikv - D(ik)^\alpha}.$$

Since in general $(ik)^\alpha \hat{f}(k)$ is the Fourier transform of the Riemann-Liouville fractional-derivative $d^\alpha f(x)/dx^\alpha$, it follows that $v\alpha C^f(x, t) + v(1-\alpha)C(x, t)$ has the same Fourier-Laplace transform as the function $vC(x, t) + D\alpha \partial^{\alpha-1} C(x, t) / \partial x^{\alpha-1}$. Then it follows that

$$v\alpha C^f(x, t) + v(1-\alpha)C(x, t) = vC(x, t) + D\alpha \frac{\partial^{\alpha-1} C(x, t)}{\partial x^{\alpha-1}},$$

which leads directly to equation (14).

A2. Derivation of Equation (15)

Next we note from Neupauer and Wilson [2002, equation (10)] that the correct load term for the backward release time equation is

$$h(x, \tau) = C^f \delta(x - x_d) \delta(\tau),$$

where $\tau = T - t$ denotes the backward time. In order to compute the Frechét-derivative term $\partial h / \partial C$ in (11), we follow Neupauer and Wilson [1999, Appendix B]. To verify the weak inequality

$$\frac{\partial}{\partial C} \left[-\frac{D \partial^{x-1} C}{v \partial x^{x-1}} \delta(x-x') \delta(t-t') \right] = \frac{D \partial^{x-1} \delta(x-x')}{v \partial(-x)^{x-1}} \delta(t-t'),$$

note that the Frechét derivative of the term in square brackets above is the operator

$$L = -\frac{D}{v} \delta(x-x') \delta(t-t') \frac{\partial^{x-1}}{\partial x^{x-1}}$$

and recall that two operators are weakly equal if the results of their operation on a test function are equal. Then just note that for a test function $\phi = \phi(x, t)$, we have

$$\begin{aligned} \langle L, \phi \rangle &= -\frac{D}{v} \int_{-\infty}^{\infty} \int_0^{\infty} \delta(x-x') \delta(t-t') \frac{\partial^{x-1}}{\partial x^{x-1}} \phi(x, t) dt dx \\ &= \frac{D}{v} \int_{-\infty}^{\infty} \int_0^{\infty} \frac{\partial^{x-1}}{\partial(-x)^{x-1}} \delta(x-x') \delta(t-t') \phi(x, t) dt dx \\ &= \langle (D/v) \partial^{x-1} \delta(x-x') / \partial(-x)^{x-1} \delta(t-t'), \phi \rangle \end{aligned}$$

using the adjoint formula (5), and this proves that equation (15) holds.

A3. Derivation of Equation (16)

Next we solve the backward FADE (11) with $q_i = 0$ and $\partial h / \partial C$ given by (15) using the method of Fourier-Laplace transforms. Take Fourier transforms in (11) to get

$$\frac{d\hat{A}}{d\tau} = v(ik)\hat{A} + D(-ik)^{\alpha} \hat{A} + e^{-ikx_d} [1 + (D/v)(-ik)^{\alpha-1}] \delta(\tau),$$

which implies that

$$\hat{A}(k, \tau) = [1 + (D/v)(-ik)^{\alpha-1}] e^{-ikx_d} \exp[v\tau(ik) + D\tau(-ik)^{\alpha}]$$

and then take Laplace transforms to get

$$\tilde{\hat{A}} = \frac{[1 + (D/v)(-ik)^{\alpha-1}] e^{-ikx_d}}{s - v(ik) - D(-ik)^{\alpha}}. \tag{A3}$$

To simplify, set $x_d = 0$ and then we will follow Zhang et al. [2006] to invert this Fourier-Laplace transform.

Zhang et al. [2006, equation (7)] shows that

$$-i \frac{\partial}{\partial k} \int_{\infty}^s \tilde{g}(k, u) du$$

is the Fourier-Laplace transform of $(x/t)g(x, t)$ for any suitable function $g(x, t)$.

Next recall that, as an abstract mathematical device, the backward FADE

$$\frac{\partial g}{\partial t} = v \frac{\partial g}{\partial x} + D \frac{\partial^2 g}{\partial(-x)^{\alpha}} + \delta(x) \delta(t), \tag{A4}$$

has Fourier transform

$$\frac{d\hat{g}}{dt} = v(ik)\hat{g} + D(-ik)^{\alpha} \hat{g} + \delta(t)$$

and hence Fourier solution

$$\hat{g}(k, \tau) = \exp [v\tau(ik) + D\tau(-ik)^\alpha],$$

and hence its Fourier-Laplace transform is

$$\tilde{g}(k, s) = \frac{1}{s - v(ik) - D(-ik)^\alpha}.$$

Now compute that

$$\begin{aligned} & -i \frac{\partial}{\partial k} \int_{-\infty}^{\infty} \tilde{g}(k, u) du \\ &= -i \int_{-\infty}^{\infty} \frac{\partial}{\partial k} \left[\frac{1}{u - v(ik) - D(-ik)^\alpha} \right] du \\ &= (-i)^2 [v - D\alpha(-ik)^{\alpha-1}] \int_{-\infty}^{\infty} \left[\frac{-1}{[u - v(ik) - D(-ik)^\alpha]^2} \right] du \\ &= \frac{-v + D\alpha(-ik)^{\alpha-1}}{s - v(ik) - D(-ik)^\alpha} \end{aligned}$$

is the Fourier-Laplace transform of $(x/t)g(x,t)$. Next use (A3) with $x_d = 0$ to write

$$v\alpha\tilde{A}(k, s) = \frac{v\alpha + D\alpha(-ik)^{\alpha-1}}{s - v(ik) - D(-ik)^\alpha} = \frac{-v + D\alpha(-ik)^{\alpha-1}}{s - v(ik) - D(-ik)^\alpha} + \frac{(1 + \alpha)v}{s - v(ik) - D(-ik)^\alpha}$$

and then invert the Fourier-Laplace transforms to see that

$$v\alpha A(x, t) = \frac{x}{t} g(x, t) + v(1 + \alpha) g(x, t).$$

Then solve to obtain

$$A(x, t) = \left[1 + \frac{x + vt}{v\alpha t} \right] g(x, t). \tag{A5}$$

In our application, we have $g(x, t) = f_x(x; t)$ (note that equation (13) with $x_d = 0$ is equivalent to (A4)), the probability density function of contaminant release location. Hence we can compute the probability density function of release time using

$$f_t(\tau; x) = vA(x, \tau) = v \left[1 + \frac{x + v\tau}{v\alpha\tau} \right] f_x(x; \tau),$$

which proves equation (16).

Acknowledgments

Y. Zhang was partially supported by the National Science Foundation (NSF) grant DMS-1460319 and University of Alabama. M. M. Meerschaert was partially supported by NSF grants DMS-1462156 and EAR-1344280 and the ARO grant W911NF-15-1-0562. This paper does not necessarily reflect the views of the funding agencies. The data used are listed in the reference [Boggs et al., 1992; Boggs and Adams, 1992] and data repository at <http://www.dtic.mil/cgi-bin/GetTRDoc?AD=ADA319756>.

References

- Adams, E. E., and L. W. Gelhar (1992), Field study of dispersion in a heterogeneous aquifer: 2. Spatial moment analysis, *Water Resour. Res.*, 28(12), 3293–3307.
- Atmadja, J., and A. C. Bagtzoglou (2001), State of the art report on mathematical methods for groundwater pollution source identification, *Environ. Forensics*, 2, 205–214.
- Benson, D. A. (1998), The fractional advection-dispersion equation: Development and application, PhD dissertation, Univ. of Nev., Reno.
- Benson, D. A., R. Schumer, M. M. Meerschaert, and S. W. Wheatcraft (2001), Fractional dispersion, Lévy motion, and the MADE tracer tests, *Transp. Porous Media*, 42, 211–240.
- Berkowitz, B., A. Cortis, M. Dentz, and H. Scher (2006), Modeling non-Fickian transport on geological formations as a continuous time random walk, *Rev. Geophys.*, 44, RG2003, doi:10.1029/2005RG000178.
- Boggs, J. M., and E. E. Adams (1992), Field study of dispersion in a heterogeneous aquifer: 4. Investigation of adsorption and sampling bias, *Water Resour. Res.*, 28(12), 3325–3336.
- Boggs, J. M., S. C. Young, and L. M. Beard (1992), Field study of dispersion in a heterogeneous aquifer: 1. Overview and site description, *Water Resour. Res.*, 28(12), 3281–3291.
- Chen, M., and W. Deng (2014), Fourth order accurate scheme for the space fractional diffusion equations, *SIAM J. Numer. Anal.*, 52, 1418–1438.
- Defterli, O., M. DElia, Q. Du, M. Gunzburger, R. Lehoucq, and M. M. Meerschaert (2015), Fractional diffusion on bounded domains, *Fractional Calculus Appl. Anal.*, 18, 342–360.
- Deng, Z.-Q., L. Bengtsson, and V. P. Singh (2006), Parameter estimation for fractional dispersion model for rivers, *Environ. Fluid Mech.*, 6, 451–475.
- Jia, X. Z., G. S. Li, C. L. Sun, and D. H. Du (2015), Simultaneous inversion for a diffusion coefficient and a spatially dependent source term in the SFADE, *Inverse Probl. Sci. Eng.*, 16, 1–28.

- Kim, S., and M. L. Kavvas (2006), Generalized Fick's law and fractional ADE for pollutant transport in a river: Detailed derivation, *J. Hydrol. Eng.*, *11*(1), 80–83.
- Liu, X., and Z. Zhai (2007), Inverse modeling methods for indoor airborne pollutant tracking: Literature review and fundamentals, *Indoor Air*, *17*, 419–438.
- Meerschaert, M. M. (2012), Fractional calculus, anomalous diffusion, and probability, in *Fractional Dynamics*, edited by R. Metzler and J. Klafter, pp. 265–284, World Sci., Singapore.
- Meerschaert, M. M., and A. Sikorskii (2012), *Stochastic Models for Fractional Calculus, De Gruyter Stud. Math.*, vol. 43, Walter de Gruyter, Berlin.
- Meerschaert, M. M., D. A. Benson, and B. Baeumer (1999), Multidimensional advection and fractional dispersion, *Phys. Rev. E*, *59*(5), 5026–5028.
- Meerschaert, M. M., Y. Zhang, and B. Baeumer (2008), Tempered anomalous diffusion in heterogeneous systems, *Geophys. Res. Lett.*, *35*, L17403, doi:10.1029/2008GL034899.
- Metzler, R., and J. Klafter (2000), The random walks guide to anomalous diffusion: A fractional dynamics approach, *Phys. Rep.*, *339*(1), 1–77.
- Metzler, R., and J. Klafter (2004), The restaurant at the end of the random walk: Recent development in fractional dynamics of anomalous transport processes, *J. Phys.*, *37*, R161–R208.
- Neupauer, R. M., and J. L. Wilson (1999), Adjoint method for obtaining backward-in-time location and travel time probabilities of a conservative groundwater contaminant, *Water Resour. Res.*, *35*(11), 3389–3398.
- Neupauer, R. M., and J. L. Wilson (2002), Backward probabilistic model of groundwater contamination in non-uniform and transient flow, *Adv. Water Resour.*, *25*, 733–746.
- Polyanin, A. D., and A. V. Manzhirov (1998), *Handbook of Integral Equations*, 787 pp., Chapman & Hall/CRC Press, Boca Raton-London, U. K.
- Rehfeldt, K. R., J. M. Boggs, and L. W. Gelhar (1992), Field study of dispersion in a heterogeneous aquifer: 3. Geostatistical analysis of hydraulic conductivity, *Water Resour. Res.*, *28*(12), 3309–3324.
- Sabzikar, F., M. M. Meerschaert, and J. Chen (2015), Tempered fractional calculus, *J. Comput. Phys.*, *293*, 14–28.
- Schumer, R., D. A. Benson, M. M. Meerschaert, and B. Baeumer (2003), Fractal mobile/immobile solute transport, *Water Resour. Res.*, *39*(10), 1296, doi:10.1029/2003WR002141.
- Schumer, R., M. M. Meerschaert, and B. Baeumer (2009), Fractional advection-dispersion equations for modeling transport at the Earth surface, *J. Geophys. Res.*, *114*, F00A07, doi:10.1029/2008JF001246.
- Shlesinger, M. F., G. M. Zaslavsky, and J. Klafter (1993), Strange kinetics, *Nature*, *363*, 31–37.
- Solomon, T. H., E. R. Weeks, and H. L. Swinney (1993), Observation of anomalous diffusion and Lévy flights in a two-dimensional rotating flow, *Phys. Rev. Lett.*, *71*, 3975–3978.
- Tadjeran, C., M. M. Meerschaert, and H. P. Scheffler (2006), A second order accurate numerical approximation for the fractional diffusion equation, *J. Comput. Phys.*, *213*, 205–213.
- Voller, V. R., V. Ganti, C. Paola, and E. Foufoula-Georgiou (2012), Does the flow of information in a landscape have direction?, *J. Geophys. Res.*, *39*, L01403, doi:10.1029/2011GL050265.
- Wang, H., and D. Yang (2013), Wellposedness of variable-coefficient conservative fractional elliptic differential equations, *SIAM J. Numer. Anal.*, *51*, 1088–1107.
- Zayernouri, M., and G. Em. Karniadakis (2014), Fractional spectral collocation method, *SIAM J. Sci. Comput.*, *36*, A40–A62.
- Zhang, Y., D. A. Benson, M. M. Meerschaert, and H.-P. Scheffler (2006), On using random walks to solve the space-fractional advection-dispersion equations, *J. Stat. Phys.*, *123*(1), 89–110.
- Zhang, Y., D. A. Benson, M. M. Meerschaert, and E. M. LaBolle (2007), Space-fractional advection-dispersion equations with variable parameters: Diverse formulas, numerical solutions, and application to the MADE-site data, *Water Resour. Res.*, *43*, W05439, doi:10.1029/2006WR004912.
- Zhang, Y., D. A. Benson, and B. Baeumer (2008), Moment analysis for spatiotemporal fractional dispersion, *Water Resour. Res.*, *44*, W04424, doi:10.1029/2007WR006291.
- Zhang, Y., D. A. Benson, and D. M. Reeves (2009), Time and space nonlocalities underlying fractional-derivative models: Distinction and literature review of field applications, *Adv. Water Resour.*, *32*(4), 561–581.
- Zhang, Y., M. M. Meerschaert, and A. I. Packman (2012), Linking fluvial bed sediment transport across scales, *Geophys. Res. Lett.*, *39*, L20404, doi:10.1029/2012GL053476.
- Zheng, C. M., M. Bianchi, and S. M. Gorelick (2011), Lessons learned from 25 years of research at the MADE site, *Ground Water*, *49*(5), 649–662.

